AWARD NUMBER: W81XWH-19-1-0257

TITLE: Leveraging Rational Nanoparticle Design for Improved Treatment of Pediatric and Adolescent Cancers

PRINCIPAL INVESTIGATOR: Natalie Boehnke

CONTRACTING ORGANIZATION: Massachusetts Institute of Technology

REPORT DATE: July 2020

TYPE OF REPORT: Annual

PREPARED FOR: U.S. Army Medical Research and Materiel Command
Fort Detrick, Maryland 21702-5012

REPORT DOCUMENTATION PAGE

Form Approved
OMB No. 0704-0188

1. REPORT DATE	2. REPORT TYPE	3. DATES COVERED
July 2020	Annual	01-Jul-2019 to 30-Jun-2020

4. TITLE AND SUBTITLE

Leveraging Rational Nanoparticle Design for Improved Treatment of Pediatric and Adolescent Cancers

5a. CONTRACT NUMBER

5b. GRANT NUMBER
W81XWH-19-1-0257

5c. PROGRAM ELEMENT NUMBER

6. AUTHOR(S)
Natalie Boehnke

E-Mail: nboehnke@mit.edu

5d. PROJECT NUMBER

5e. TASK NUMBER

5f. WORK UNIT NUMBER

7. PERFORMING ORGANIZATION NAME(S) AND ADDRESS(ES)
Koch Institute for Integrative Cancer Research at MIT

500 Main Street
Cambridge, MA 02139

8. PERFORMING ORGANIZATION REPORT NUMBER

9. SPONSORING / MONITORING AGENCY NAME(S) AND ADDRESS(ES)

U.S. Army Medical Research and Development Command
Fort Detrick, Maryland 21702-5012

10. SPONSOR/MONITOR'S ACRONYM(S)

11. SPONSOR/MONITOR'S REPORT NUMBER(S)

12. DISTRIBUTION / AVAILABILITY STATEMENT

Approved for Public Release; Distribution Unlimited

13. SUPPLEMENTARY NOTES

14. ABSTRACT
The **purpose** of this proposal is to utilize a high-throughput pan-cancer screening approach (PRISM) to identify effective therapeutic nanoparticle formulations for the treatment of cancers found in children, adolescents, and young adults. The **scope** of the project reported herein comprised 1) the synthesis and characterization of a library of fluorescently-labeled nanoparticles with diverse surface chemistries, including tumor targeting and penetrating peptide motifs, 2) profiling of nanoparticle-cell associations via flow cytometry in a select number of cell lines, originating from patients classified as children, adolescents, or young adults, and 3) the screening of this nanoparticle library via the PRISM platform to identify comprehensive data on the structure–function relationship between nanoparticles and specific cell types, elucidate uptake trends across specific lineage sub-analyses, as well as highlight differences in nanoparticle uptake in pediatric, adolescent, and adult cancer cell lines. The **major findings** resulting from this work include development and validation of the flow-based PRISM screen to sort and analyze nanoparticle-cell interactions through the use of correlative genomics, the identification of the predominant nanoparticle parameters driving particle-cancer cell interactions, evaluation of the effects of cancer cell line lineage and doubling time on nanoparticle uptake, and the identification of a nanoparticle-specific biomarker that can be used to predict the propensity of a cancer cell to take up nanoparticles as well as the extension of these findings to cell lines derived from patients classified as children, adolescents, and young adults, with specific emphasis on nervous system and bone cancers.

15. SUBJECT TERMS

16. SECURITY CLASSIFICATION OF:			17. LIMITATION OF ABSTRACT	18. NUMBER OF PAGES	19a. NAME OF RESPONSIBLE PERSON
a. REPORT	b. ABSTRACT	c. THIS PAGE			USAMRMC
Unclassified	Unclassified	Unclassified	Unclassified		19b. TELEPHONE NUMBER *(include area code)*

TABLE OF CONTENTS

1. INTRODUCTION:

Until recently, the only rigorous way to validate targeted therapies, such as NPs, involved establishing multiple cancer cell lines and carrying out extensive *in vitro* and *in vivo* screening. This is a massive undertaking of time and resources, is unlikely to capture the heterogeneity of a pan-cancer screen, and presents a particular challenge for cancers affecting pediatric, young adult, and adolescent patients that have limited and/or difficult to culture cell lines. This encompasses the **subject** of the research. PRISM, a collaborative platform available to the broader MIT scientific community, leverages pooling of stably DNA-barcoded cell lines to profile compounds across hundreds of cancer cell lines in a single assay. The **purpose** of the research described herein is to utilize this high-throughput pan-cancer screening approach to identify effective therapeutic nanoparticle formulations for the treatment of cancers found in children, adolescents, and young adults through the use of correlative genomics. The **scope** of the project reported herein comprised 1) the synthesis and characterization of a library of fluorescently-labeled nanoparticles with diverse surface chemistries, including tumor targeting and penetrating peptide motifs, 2) profiling of nanoparticle-cell associations via flow cytometry in a select number of cell lines, originating from patients classified as children, adolescents, or young adults, and 3) the screening of this nanoparticle library via the PRISM platform to identify comprehensive data on the structure–function relationship between nanoparticles and specific cell types, elucidate uptake trends across specific lineage sub-analyses, as well as highlight differences in nanoparticle uptake in pediatric, adolescent, and adult cancer cell lines.

2. KEYWORDS:

Nanoparticle, layer-by-layer, tumor targeting, pediatric, adolescent, young adult, cancer, genomics, omics, DNA barcodes, pooled screen

3. ACCOMPLISHMENTS:

What were the major goals of the project?

Specific Aim 1. A library of NPs with diverse surface chemistry families will be generated.

- Major Task 1. Generate LbL-NP library
  - Milestone: LbL-NP library completed
    - Projected timeline: 3 months (Oct. 2019)
    - Actual completion date: September 2019
    - Percentage completion: 100%
- Major Task 2. Incorporate tumor targeting ligands into LbL-NP library
  - Milestone: Tumor targeting LbL-NP library completed
    - Projected timeline: 3 months (Oct. 2019)
    - Actual completion date: Feb. 2020
    - Percentage completion: 100%

Specific Aim 2. Examine structure-function relationship of NP surface chemistry on particle uptake.

- Major Task 1. Identify and culture three representative cell lines from PRISM platform for preliminary *in vitro* screening
  - Milestone: IRB (called Biological Research Registration at MIT), EHS, and HRPO approval
    - Projected timeline: 3 months (Oct. 2019)
    - Actual completion date: May 2019 (BRR approval, title of registration: 584: Nanoparticles as new targeted delivery systems)
    - Note: Use of CCLE characterized cell lines, including the ones used in this work, does not require HRPO review and approval.
  - Milestone: Cells and culture conditions identified for preliminary NP dosing screens. The 3 selected sarcoma and nervous system cancer cell lines will be selected from the PRISM pool based on commercial availability, ease of culture, and origin from young patients.

        - Projected timeline: 4 months (Nov. 2019)
        - Actual completion date: August 2019
        - Percentage completion: 100%

- Major Task 2. Preliminary *in vitro* (non-high throughput) testing to determine fluorescent NP dosing conditions
    - Milestone: NP dosing conditions determined for PRISM screen
        - Projected timeline: 5 months (Dec. 2019)
        - Actual completion date: October 2019
        - Percentage completion: 100%

- Major Task 3. Perform PRISM screen using LbL-NP library
    - Milestone: Four optimal NP surface chemistries identified (two pan-cancer, two tumor type-specific: blastoma and sarcoma).
        - Projected timeline: 7 months (Feb. 2020)
        - Actual completion date: June 2020
        - Percentage completion: 100%

Specific Aim 3. Examine structure-function relationship of NP surface chemistry on therapeutic efficacy.

- Major Task 1. Synthesize cisplatin-loaded versions of the four NPs identified from the screen in aim 2.
    - Milestone: Mini cisplatin-loaded NP library prepared
        - Projected timeline: 8 months (March 2020)
        - Actual completion date: ongoing
        - Percentage completion: 15%

- Major Task 2. Perform preliminary *in vitro* cytoxicity studies using the three identified cell lines
    - Milestone: Cisplatin-loaded NP efficacy confirmed.
        - Projected timeline: 9 months (April 2020)
        - Actual completion date: ongoing
        - Percentage completion: 0%

- Major Task 3. Perform PRISM screen using cisplatin- loaded NPs.
    - Milestone: Data correlating nanoparticle uptake, therapeutic efficacy and particle surface chemistry will be obtained to aid in future design and testing of therapeutic NPs for underexplored cancers affecting children, adolescents, and young adults.
        - Projected timeline: 12 months (July 2020)
        - Actual completion date: Ongoing
        - Percentage completion: 50% (correlative data obtained in aim 2 has already contributed towards completion of this milestone)

What was accomplished under these goals?

Specific aim 1, major task 1:
Specific objective: generate LbL-NP library

Major activities, significant results, and key findings:
Due to material and experimental constraints (described in greater detail under specific aim 2), we determined that a total of 40 different formulations (including antibody and untreated controls) could be used to screen against the 500 pooled, adherent cancer cell lines available from PRISM.

A lipid mixture composed of 31 mol% DSPC, 31 mol% cholesterol, 31 mol% DSPG and 6 mol% DSPE (for covalent dye modification) was employed for the base liposome formulation. These liposomes were electrostatically coated with cationic poly-L-arginine (PLR) as well as a series of polyanions. The polyanionis were selected for their synthetic (polyacrylic acid, PAA), semisynthetic (poly-L-aspartate PLD, poly-L-glutamate PLE), or natural (hyaluronate (HA), dextran sulfate (DXS), fucoidan (FUC), alginate (ALG), chondroitin sulfate (CS)) origin as well as the inclusion of both carboxylate and sulfate ions. These same electrostatic coatings were used to modify polymeric nanoparticle cores (polylactide-co-glycolide, PLGA), containing non-covalently incorporated hydrophobic fluorescent dye, in order to test the effects core composition may have on NP-cell interactions. Additionally, PEGylated versions of both liposome and PLGA particles were prepared, including the drug-free versions of two commercial liposome formulations, Doxil and Onivyde. Dynamic light scattering (DLS) was used to characterize the diameter and dispersity (Figure 1) and zeta potential (Figure 2) of this NP library.

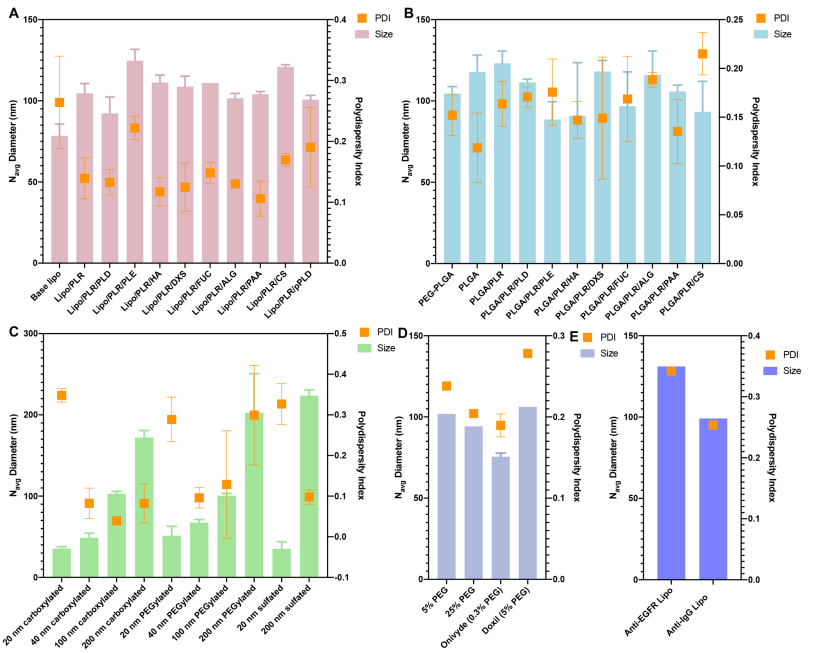

Figure 1. Size and dispersity of nanoparticle library utilized in PRISM screen as characterized by dynamic light scattering.

Additionally, an antibody was selected as a downstream sorting control to ensure that binning pooled cancer cells by increasing NP associated fluorescence would result in correct and meaningful data. Therefore, an anti-EGFR antibody (nonlethal) was selected and fluorescently labeled or covalently incorporated onto a fluorescent liposome using a standard coupling protocol provided by the manufacturer. An IgG isotype was modified in the same manner to serve as a negative control.

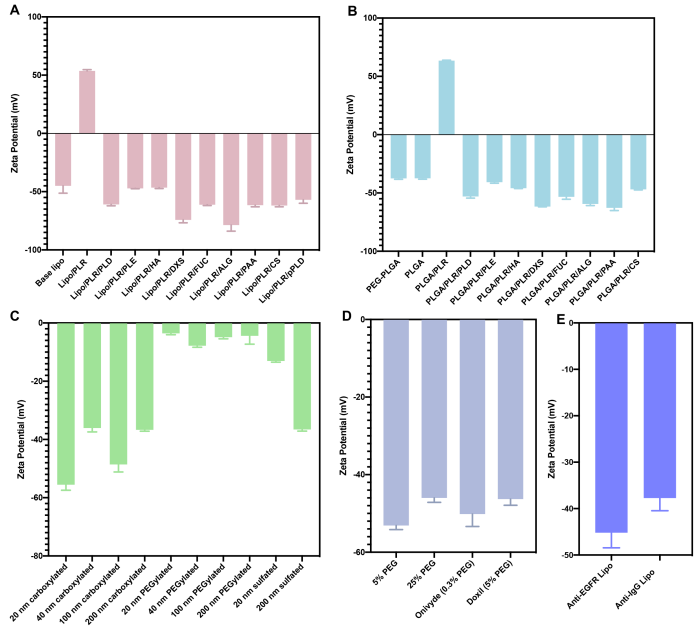

Figure 2. Zeta potential measurements of nanoparticle library utilized in PRISM screen as characterized by dynamic light scattering.

Specific aim 1, major task 2:
Specific objective: Incorporate tumor targeting ligands into LbL-NP library

Major activities, significant results, and key findings:

Tumor penetrating and targeting peptides were selected and incorporated onto NP surfaces in two different methods. Using copper catalyzed click chemistry conditions previously established in the Hammond lab, iRGD, a neutral targeting peptide that interacts with integrins on the surfaces of cancer cells, was covalently attached.[1] Because covalent modification of NP surfaces with targeting ligands requires easy-to-functionalize chemical handles, this approach is limited to a smaller subset (e.g. carboxylated) surface coatings. We conjugated azide-modified iRGD to propargyl modified PLD (pPLD) NPs as we have previously shown this to result in improved delivery to ovarian cancer cells *in vitro* as well as *in vivo*, and we hypothesized that we would see similar uptake enhancements in the pooled PRISM screen of cell lines with integrin overexpression.

We additionally incorporated cationic tumor penetrating peptides (TPPs) LyP-1 and LinTT1, established to interact with p32, a receptor overexpressed on the surface of cancer cells, onto our anionic LbL NPs by taking advantage of the noncovalent charge-based interactions between peptide and NP. To this end, we modified PLD, PLE, HA, and DXS LbL liposomes with both cationic peptides, and characterized the stability of the particles to peptide adsorption and purification (Figure 3).

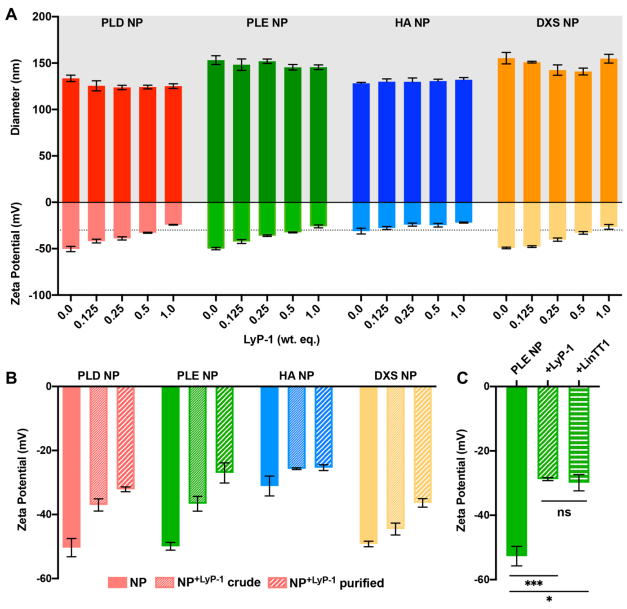

Figure 3. (**A**) Effects of LyP-1 titration in dilute HEPES onto the LbL NP library on particle size and zeta potential were monitored using dynamic light scattering. The -30 mV charge threshold for colloidal stability is indicated by a dashed line. (**B**) The zeta potential was measured before and after adsorption of 0.25 wt. eq. LyP-1 onto the LbL NP library as well as after purification of the modified NPs via tangential flow filtration. (**C**) Zeta potential measurements of PLE NPs after LyP-1 and LinTT1 adsorption (0.2 wt. eq.) and purification to remove unadsorbed peptide indicate similar interactions between the two peptides and the NP. Error bars represent the standard deviation of three measurements. * $p < 0.05$, *** $p < 0.005$, determined using Student's t test.

Peptide loading of the LbL NP library post-purification was assessed using a fluorometric assay. Because Lyp-1 is a cyclic disulfide, we chose to use a probe that could quantify resulting thiol groups following reduction of LyP-1 with tris(2-carboxyethyl)phosphine (TCEP). To quantify LinTT1, a thiolated derivative containing an N-terminal cysteine was synthesized (LinTT1-SH). Using this probe, ABD-F, we determined the % peptide retention corresponded to high peptide loading, ranging from 3700 to 8400 LyP-1 molecules per NP. Specifically, PLD NPs retained 53.5±0.3%, PLE NPs retained 48.6±0.9%, HA NPs retained 80.5±1.0%, and DXS NPs retained 110±2.5% of the 0.2 wt. eq. LyP-1. DXS NPs retained much higher amounts of LyP-1 than the tested carboxylated LbL NPs. We attribute this to the stronger binding of the sulfate groups with the cations present in LyP-1. The two polysaccharide coated NPs retained higher amounts of LyP-1 than the polypeptide coated NPs. This could be due to increased hydrogen bonding capabilities of the sugar backbones with the peptide ligands compared to the polypeptides. Similar loading was observed for LinTT1-SH containing NPs.

As solution conditions are critical for colloidal LbL stability and retention of cargo, we compared the adsorption of LyP-1 onto LbL NPs in water, dilute HEPES (1 mM, pH 7.4. for slight pH buffering), as well as 25 mM HEPES + 20 mM NaCl (pH 7.4, for pH control and charge shielding)24 (Figures 2A, S3A). We found that 0.5 wt. eq. LyP-1 was stably incorporated onto the LbL NP surfaces in both the HEPES and HEPES + NaCl solution conditions, indicating the presence of slight buffering conditions improves LyP-1 adsorption. Conversely, adsorption of LyP-1 in water resulted in particle aggregation at this concentration. However, at a lower wt. eq. of LyP-1, all solution conditions resulted in stable NPs with no difference in particle functionality.

We evaluated the stability of peptide interactions with NP surface to increasing salt (NaCl) concentrations. For colloidal LbL NPs, layers are built up primarily through charge-charge interactions in combination with secondary interactions. The same premise applies for TPP adsorption onto the NP surface, though these interactions are fewer because of the peptides' lower net charge compared to polyelectrolytes. Therefore, we hypothesized that if the peptides were only weakly or transiently associated with the NP surface, dilute amounts of NaCl would disrupt these non-covalent interactions through excess shielding, detectable via a change in NP diameter or ζ. We first established the stability of PLE and DXS NPs to NaCl and found that they were stable to 50 and 100 mM NaCl, respectively. At and above these NaCl concentrations, loss of colloidal stability was observed either through particle aggregation (indicated by a significant increase in measured particle size in DLS) or reduction of ζ. Addition of 0.5 wt. eq. LyP-1 onto these NPs did not change the colloidal stability from what was observed for the NPs without LyP-1 (Figure 4A). Moreover, ζ measurements for PLE NP+LyP-1 and DXS NP+LyP-1 read consistently less negative than PLE NP and DXS NP counterparts up to the point of general particle destabilization, indicating that the LyP-1 NP interactions are as stable as the electrostatically assembled LbL NPs.

PLE NP+LinTT1-SH and DXS NP+LinTT1-SH destabilized at lower salt concentrations of 5 and 50 mM NaCl, respectively, pointing to the presence of LinTT1 having a disruptive effect on NP stability. Because the two TPPs exhibit the same overall net charge (+3) as well as similar molecular weights and polar surface areas, we hypothesized that structural differences, specifically cyclic vs. linear, between the two peptides may explain the observed differences.

As we are pioneering this new NP surface modification approach, we elected to carry out comprehensive *in vitro* validation experiments using the high grade serous ovarian cancer cell line, OVCAR8. While this cell line is not derived from a pediatric, adolescent, or young adult cancers, it is included in the PRISM pool. More importantly, this cell line was selected for validation studies due to its confirmed p32 expression levels[2] and prior experience in the Hammond lab, enabling comparisons to prior data and LbL NP formulations. This work was recently submitted for publication.

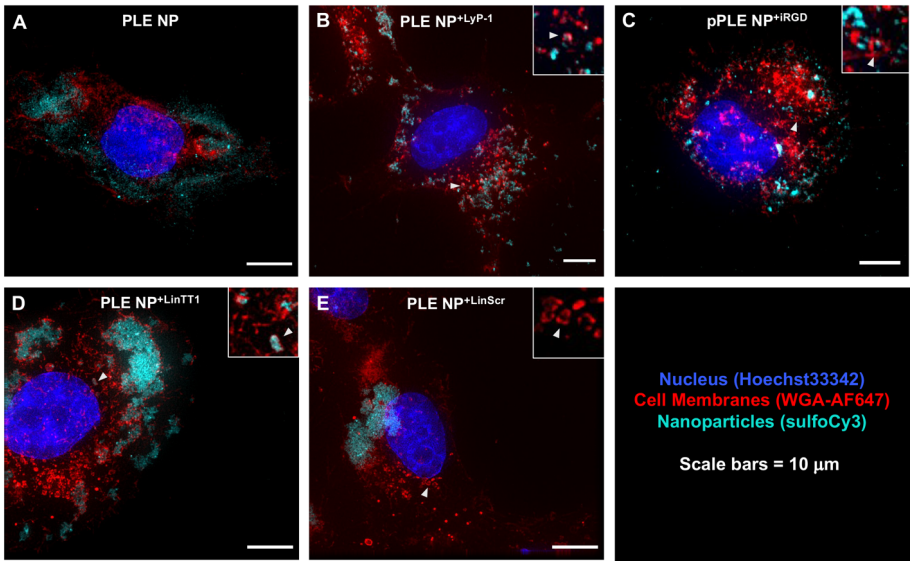

Figure 4. Deconvolution microscopy analysis of OVCAR8 cells treated for 24 with (A) PLE NPs, (B) PLE NPs+LyP-1 (C), pPLE LbL NPs+iRGD, (D) PLE NPs+ LinTT1, and (E) PLE NPs+ScrTT1. 0.3 wt. eq. of each peptide were adsorbed, with the exception of panel C, in which case an equivalent amount of iRGD was utilized.

OVCAR8 cells were dosed with fluorescently labeled NPs for 24 hours prior to fixing, staining, and imaging via deconvolution microscopy. PLE NPs were extracellularly associated on the OVCAR8 cell membranes with little to no internalization observed, consistent with our previously published findings (Figure 4A). PLE NP+LyP-1 on the other hand was efficiently internalized, colocalizing with intracellular vesicle membranes, though some of the NPs were still retained on the cell surface (Figure 4B). This indicates that function of LyP-1 is retained when adsorbed onto the NP surface in addition to the NP surface chemistry characteristics. Several control NPs were generated to rule out that observed NP internalization was not simply due to modulation of NP surface charge, including pPLE NPs+iRGD and PLE NPs adsorbed with a scrambled peptide version of LinTT1 (LinScr) (Figure 4C,E). No NP internalization was observed for these NP conditions. PLE NP+LinTT1 were internalized, though to a lesser extent than PLE+LyP-1 (Figure 4D). We also noted large patches of NP on the cell surface, and attribute this to the potential self-aggregating effect of LinTT1 on LbL NPs that we had seen previously at physiological salt conditions. This ultimately indicated that TPPs adsorbed onto the surface of PLE NPs retain their bioactivity.

Future planned work includes testing how LyP-1 and LinTT1 modified NPs are taken up by pediatric and adolescent cancer cell lines, including DAOY, U87MG, and RDES, correlating uptake trends with p32 expression levels. Additionally, it is anticipated that this broadly applicable NP functionalization technique will be useful for enhancing blood brain barrier (BBB) penetration of NPs through the adsorption of cationic shuttle peptides.

Specific aim 2, major tasks 1 and 2:
Specific objective: Identify and culture three representative cell lines from PRISM platform for preliminary *in vitro* screening and carry out preliminary *in vitro* (non-high throughput) testing to determine fluorescent NP dosing conditions

Major activities, significant results, and key findings:
Three cell lines were selected, purchased (ATCC), and cultured for preliminary *in vitro* screening to identify proper dosing and flow cytometry settings for the larger scale PRISM screen. To this end, U87MG (glioblastoma), DAOY (4 year old patient, medulloblastoma), and RDES (19 year old patient, Ewing sarcoma) were selected their origin as pediatric/adolescent cancers as well as their inclusion in the PRISM cell line pool at the time of

purchase. Cy5 labeled liposomes and PLGA NPs were functionalized with various surface coatings (PEGylation, LbL films) and used to treat these cell lines for 4 and 24 hours (time points to match downstream PRISM dosing times) prior to flow cytometry analysis. Because this experiment was designed to identify and optimize conditions, an abbreviated NP library comprised of liposomes with 5 and 25% PEG, and liposomes and PLGA NPs layered with PLD, PLE, HA, and DXS were utilized. Appropriate NP dosing volumes and time points (4 and 24 hours) were determined from these experiments.

Specific aim 2, major task 3 and specific aim 2 major task 3:
Specific objective: Perform PRISM screen using LbL-NP library and carry out correlative genetic analysis.

Major activities, significant results, and key findings:
To prepare for the pooled screen of 500 pooled, adherent cancer cell lines available from PRISM, several smaller scale pilot experiments were carried out to determine the appropriate seeding density of pooled cells (to ensure sufficient representation of each cell line for downstream DNA barcode sequencing) and establish an efficient workflow (cell plating, dosing, sorting, lysate preparation and handoff to PRISM team for barcode amplification and sequencing). As a result, we determined that the provided PRISM cells would be sufficient to screen up to 40 NP formulations at two different time points (4 and 24 hours) with three biological replicates. Because we were constrained to a limited number of NPs to test in this experiment, we elected to test LbL NPs containing two different core materials (liposomal vs. polymeric) to decouple the effects core composition may have on NP-cell interactions. We also included pre-manufactured, fluorescently labeled polystyrene beads (FluoSpheres, ThermoFisher) due to their availability in different sizes (20, 40, 100, 200 nm) and different surface chemistry presentation (carboxylated vs. sulfated). The carboxylated beads were PEGylated to evaluate the effects of anti-fouling polymers (PEG) on NP-cell interactions. For this reason, PEGylated counterparts of liposomal formulations were also included, both as derivatives of the base liposome used for LbL NP generation (5 and 25 mol% PEG incorporation) and drug-free versions of clinical liposome formulations (Doxil at 5% PEG, Onyvide at 0.3% PEG). To evaluate the effects of tumor targeting peptides on NP-cell associations, pPLD layered liposomes were prepared and iRGD was covalently incorporated via copper catalyzed click chemistry.

The pooled PRISM cells were plated and allowed to adhere for 24 hours (37 °C, 5% CO_2) prior to dosing with the NP library described in specific aim 1. NP dosing was held constant to the same mass amount per formulation (e.g. the same volume of the same concentration) per well to ensure standardization across the differing

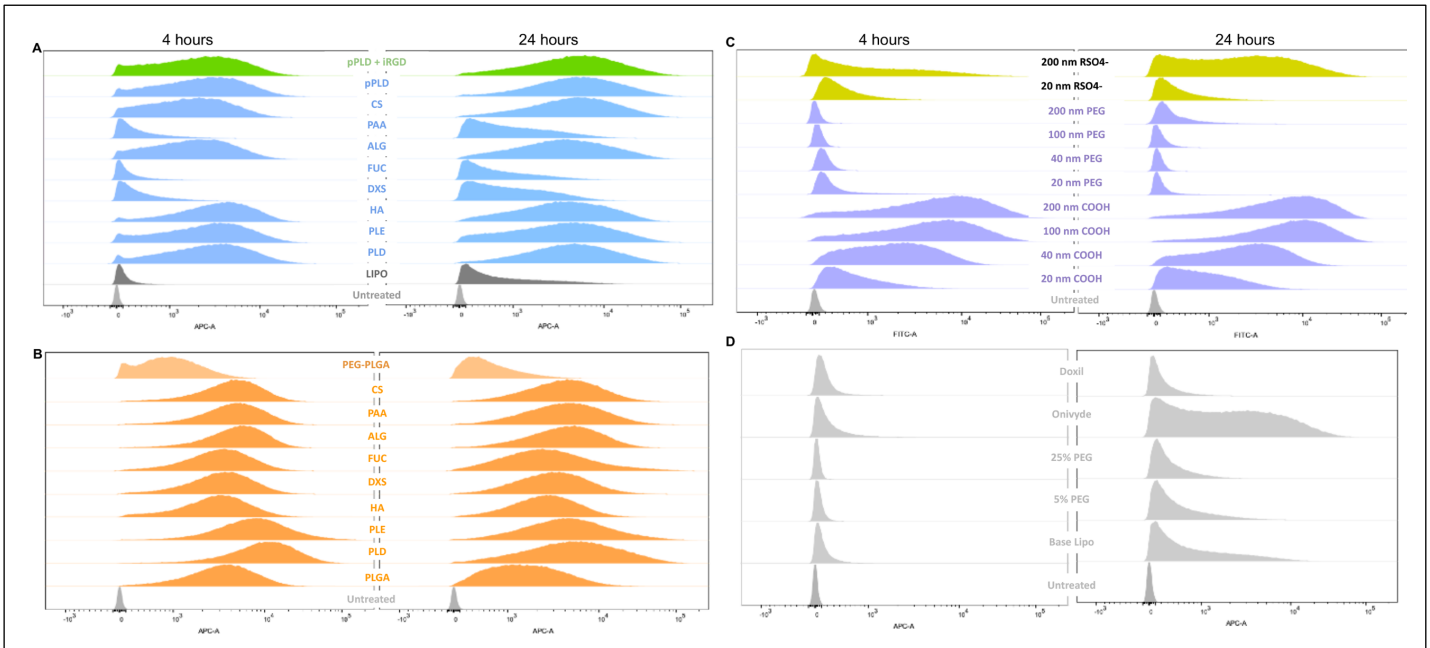

Figure 5. Flow cytometry was used to assess NP-cell interactions of (A) liposomal formulations, (B) PLGA formulations, (C) polystyrene formulations, and (D) PEGylated liposomal formulations, represented here as histograms.

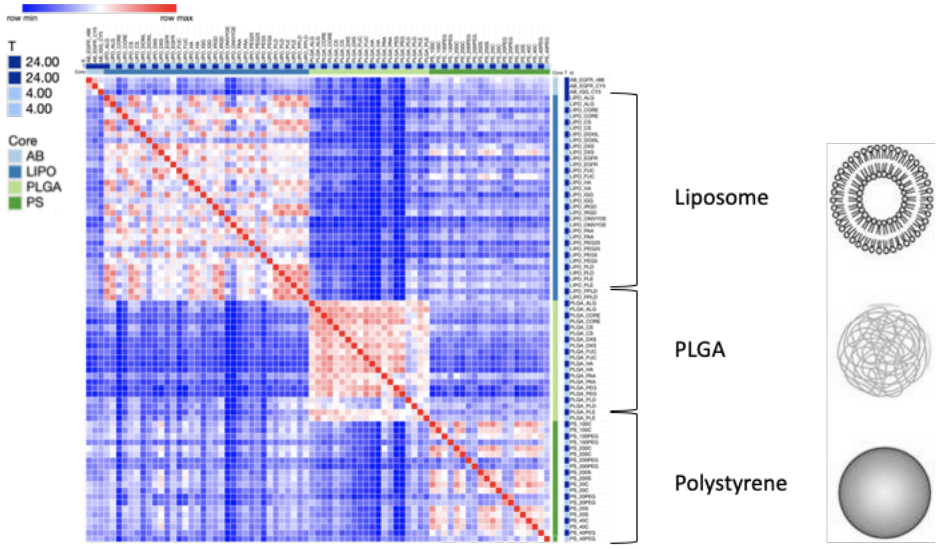

Figure 6. The WAs for each NP formulation were collapsed down and represented as a heatmap, illustrating the differences (blue) and similarities (red). Natural clusters based on NP core material are evident.

formulations containing a range of materials and fluorophores. Cells were detached via trypsin and transferred to FACS tubes. During cell sorting, a live gating strategy was employed to sort cell populations into four bins (quartiles, A, B, C, D) based on low, low-med, med-high, and high fluorescence signal (Figure 5). The cells were sorted into PRISM lysate buffer, enabling efficient transfer of cell solution to the PRISM team for DNA barcode amplification, sequencing, and preliminary data analysis.

In collaboration with PRISM, a corrective Poisson model was developed and applied to the data to account for baseline differences in barcode representation between unsorted and sorted cell populations. Data output is a probability (P) that each cell line will be found in a particular bin of each formulation, such that $P_A + P_B + P_C + P_D = 1$. After this analysis, 12 of the 500 tested cell lines were excluded for poor barcode representation or low agreement within biological replicates. This output of the remaining 488 cell lines was then utilized to calculate single value weighted averages (WA) for each NP-cell line pair: $WA = -\alpha P_A - P_B + P_C + \alpha P_D$. An α value was assigned to bins A and D to weight the lowest and highest uptake bins more heavily. Various values for α up to 100 were initially investigated, but we found that this did not affect the results of our analyses, and therefore $\alpha = 2$ was used for the data shown below.

Comparison of WA values across the tested formulations revealed natural clusters based on base/core NP formulation (e.g. liposomal, PLGA, PS) (Figure 6). This result was unexpected in that we had hypothesized surface chemistry to be a larger predictor of NP-cell interactions (e.g. carboxylated NPs or layered NPs cluster together). Principal component analysis (PCA) confirmed these formulation specific trends at both time points (Figure 7). Sub-analyses of formulation groups (e.g. liposomal based NPs) did reveal surface chemistry dependent trends, though they were more subtle than core-based clustering.

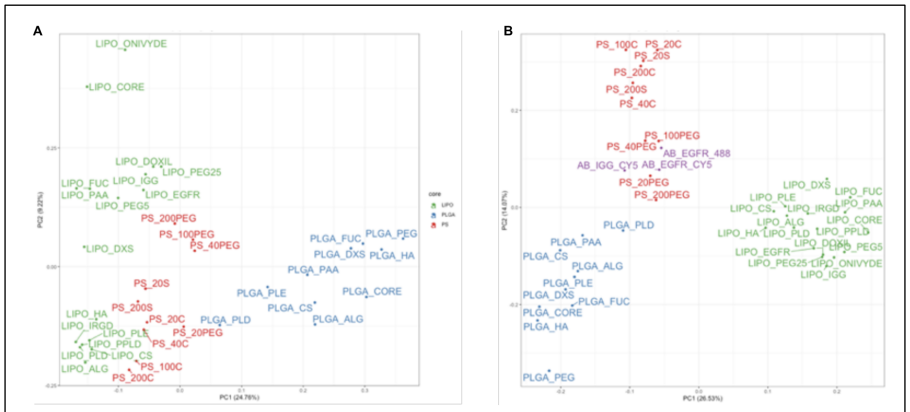

Figure 7. Principal component analysis confirms formulation-based clusters at (A) 4 and (B) 24 hour time points.

As we are interested in identifying NP formulations with specific, or preferential, interactions with certain cancer cell types (lineages) and sub-classifications of pediatric, adolescent, and young adult cancers, we also evaluated the relationship between NP-cell association and cancer cell lineage (Figure 8). PCA revealed no strong correlations between NP uptake and lineage. While this finding was initially unexpected, having hypothesized that certain cancer types might have preferential interactions with specific NP formulations, it only indicates that lineage is not a main predictor of NP uptake, and there may be underlying genetic components that still drive specific uptake of NPs. Identification of such genetic differences would enable the discovery of NP-predictive biomarkers as well as the construction of core trafficking networks. This information could then be applied to specific cancer subtypes for rational NP design.

To this end, we employed both univariate and random forest analyses (gene expression, copy number, dependency, mutations, RPPA, and miRNA). To ensure our workflow and data analysis methodology were valid, we first analyzed our validation compound (anti-EGFR and IgG isotype control) data. Both methods of analysis were able to identify the appropriate validation compound (anti-EGFR) biomarker (EGFR, gene expression and RPPA databases). EGFR was not identified in the IgG isotype-treated groups. Having confirmed the validity of our analytical approach, we evaluated the number of correlated hits (biomarkers) by significance level for each tested formulation, focusing our efforts on liposomal and polystyrene (PS) formulations as these had the highest number of significant hits at both the 4- and 24-hour time points (Figure 9). We believe that large numbers of significantly correlated hits are meaningful in the context of evaluating NP-cell interactions because NP recognition, binding, and uptake are complex cellular processes that are regulated by multiple genes and require large numbers of proteins. From this analysis, we gained a global overview of the number of biomarkers associated with specific NP formulations, and several trends emerged. First, liposomal formulations generally had mor e biomarkers associated with the earlier time point, consistent with active uptake mechanisms that result in rapid NP uptake. Second, PEGylation of both liposomal and PS formulations resulted in a drastic reduction in biomarker hits, particularly at the 4-hour time point. This was an expected result as PEG acts as an anti-fouling coating that is established to repel protein adsorption, minimizing interactions between PEGylated NPs and cell surface receptor proteins responsible for NP binding and uptake.[3]

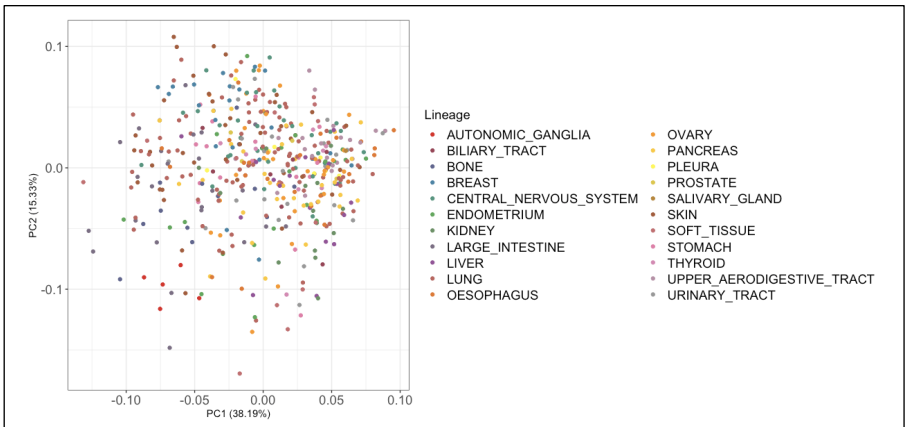

Figure 8. Principal component analysis indicated no strong correlations between NP uptake and cancer cell lineage.

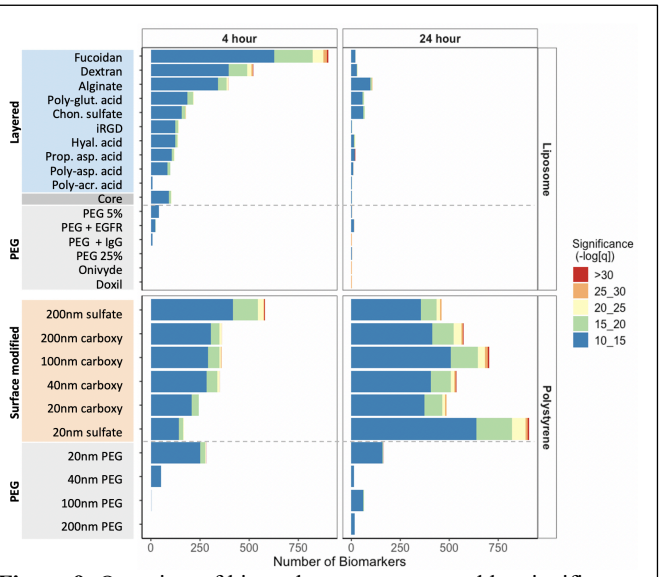

Figure 9. Overview of biomarker counts grouped by significance level of liposomal and polystyrene formulations.

Consistent with our observation that biomarker numbers may be enriched at the early time point due to active recognition and binding processes, random forest analysis of our formulations and available features annotated in the Cancer Cell Line Encyclopedia (CCLE) revealed many cell surface proteins and transporters as the most significantly enriched biomarker at this time point (Figure 10A).

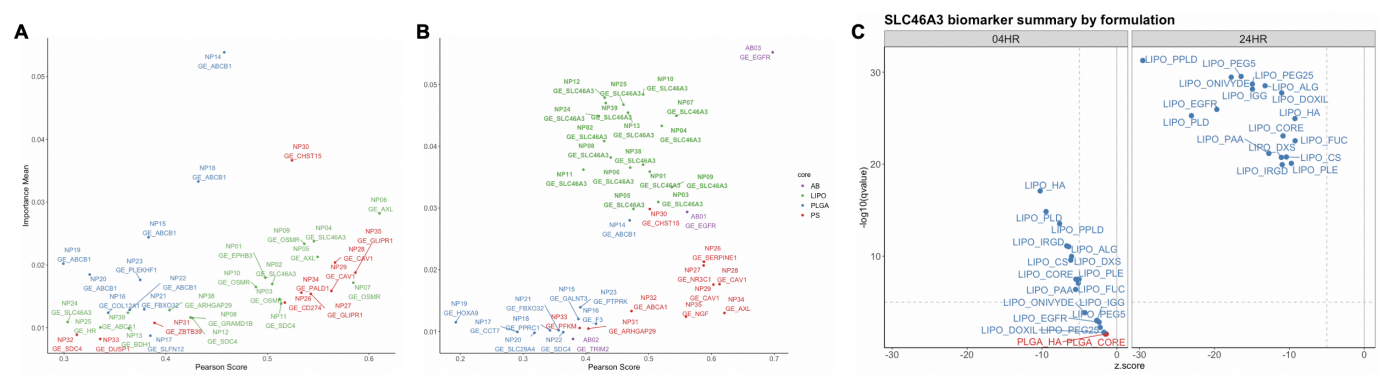

Figure 10. Random forest analysis of formulations at (A) 4- and (B) 24-hour time points reveals the top most strongly correlated CCLE feature (gene expression, GE) associated with each NP formulation. (C) Univariate analysis confirmed the random forest analysis and also provides directionality of the correlation.

Interestingly, the same analysis carried out at the 24-hour time point revealed a different trend, wherein formulations now clustered and all liposomal formulations shared the same top hit: a solute carrier protein, SLC46A3 (Figure 10B). Univariate analysis of NP formulations at both time points confirmed the random forest analysis and also indicated that the SLC46A3 was inversely correlated with NP uptake, and that this relationship was particularly strong at the later time point (Figure 10C). The protein encoded by this gene is a member of a transmembrane protein family that transports small molecules, including antibody-drug conjugates, across lysosomal membranes.[4, 5] However, because we observed inverse correlation between expression of this SLC and NP uptake, our data did not point to direct involvement of SLC46A3 with NP trafficking. Instead, as downregulation of SLC46A3 in hepatocellular carcinoma and breast cancer has been associated with a more aggressive phenotype, therapy resistance, and EMT, we hypothesize that our data indicates a potential cell state that enables certain cancer cell types to have a greater propensity to take up NPs.[6, 7]

To determine if this identified biomarker can be applied to cancer types that commonly affect younger patients, we first ranked nervous and bone cancer cell lines included in our nanoPRISM screen by SLC46A3 expression levels (DepMap, Broad Institute) and annotated the patient ages at time of sampling as well as cancer subtypes (Figure 11). Particularly for the nervous system cancers, cell lines originally obtained from patients classified as a child (0-14y), adolescent (15-24y), or young adult (16-39y) had SLC46A3 expression levels ranging from low to medium (Figure 11A). Moreover, looking at the cancer subtypes present in our screened nervous system cancer cell lines, we observed low SLC46A3 expression values for neuroblastoma and medulloblastoma lines originating from young patients (Figure 11C). The same observations held true for bone cancer cell lines, particularly for Ewing sarcoma lines (Figure 11D). We further evaluated SLC46A3 expression levels to the weighted averages obtained for the bare liposomal formulation in central nervous system cancer cell lines and cancer cell lines derived from patients less than 14 years of age to evaluate if lower SLC expression levels resulted in higher uptake of NPs as hypothesized (Figure 12). Indeed, we found a moderately strong negative correlation values between WA and SLC46A3 expression levels of -0.667 and -0.685 for central nervous system and pediatric cancer cell lines, respectively.

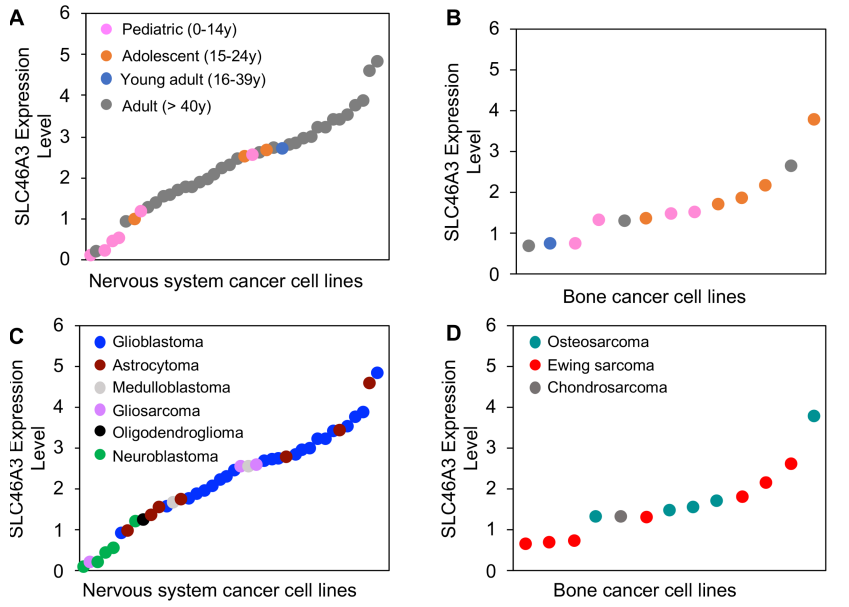

Figure 11. Ranking of (A) nervous system and (B) bone cancer cell lines included in nanoPRISM screen by their SLC46A3 expression levels. Individual cell lines are indicated by the circles and color coded by age classification of the patient at time of sampling. The same ranking was also color coded to indicate the specific cancer subtypes included in the analyzed (C) nervous system and (D) bone cancer cell lines.

Taken together, these findings suggest that our newly identified biomarker, SLC46A3, may be useful in classifying cancers in young patients by their propensity to take up nanoparticles. Specifically, we have identified that this biomarker may be predictive of liposomal nanoparticle uptake in cancers with low SLC46A3 expression levels, including those affecting children, adolescents, and young adults. Current efforts are focused on single cell line validation, using cell lines with SLC expression levels ranging from low to high. This will enable us to not only verify our findings but will also enable us to evaluate which specific liposomal formulations (e.g. LbL liposomes) result in the highest SLC64A3-dependent uptake. This validation can further be expanded to include cancer cell lines obtained from patients less than 40 years of age. The data gained from the work described in this report will additionally provide the preliminary data required to propose and carry out

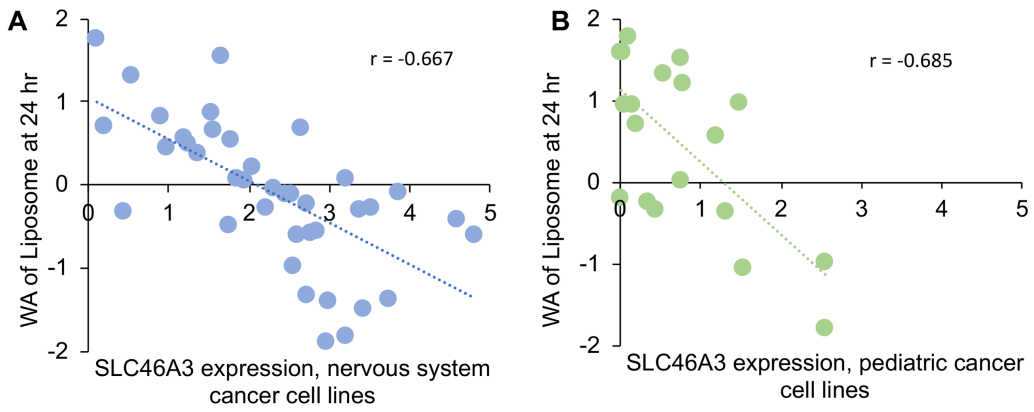

Figure 12. SLC46A3 expression levels plotted against weighted averages of the bare liposomal formulation at the 24-hour time point in (A) nervous system and (B) pediatric (0-14y) cancer cell lines indicate a moderately strong correlative

in vivo validation studies in murine cancer models with the ultimate goal of being able to utilize the identified biomarker in the clinic to stratify cancer patients by propensity to nanoparticle uptake.

Specific aim 3, major task 1.
Specific objective: Synthesize cisplatin-loaded versions of four NPs identified from the screen in aim 2.

Major activities, significant results, and key findings:
As we have identified a potential biomarker to stratify cancers based on their propensity for liposomal NP uptake, our drug-loading efforts have focused on the generation of cisplatin-loaded liposomes. Liposomes are well established for cisplatin encapsulation and delivery, and we have established encapsulation protocols (via passive loading) and quantification methods via HPLC and ICP. Instead of generating four cisplatin-loaded formulations, as proposed initially, we will instead generate cisplatin loaded versions of a range of the liposomal formulations shown in Figure 1A,D. This will enable us to screen the effects of a wider range of surface modifications on liposomal uptake and cisplatin delivery and efficacy.

What opportunities for training and professional development has the project provided?

Training:
The PI received ongoing one-on-one mentoring from her advisor, Prof. Hammond, during the report period. This mentoring was carried out in person, as well as virtually once on-campus research shut down in March, on approximately a monthly basis. Mentoring included discussions on experimental planning, data analysis, as well as strategies for how to most effectively communicate this research to the broader scientific community comprised of multiple scientific disciplines (e.g. chemistry, cancer biology, materials science, chemical and biological engineering). Additionally, Dr. Boehnke had biweekly meetings with Dr. Joelle Straehla, an Instructor at the Dana Farber Cancer Institute (DFCI)/Boston Children's Hospital (BCH) with a focus on pediatric hematology/oncology who is also a postdoc in the Hammond lab. During these meetings, research findings were discussed in the context of clinical relevance to pediatric cancers. As a result of the PRISM platform collaboration, Dr. Boehnke had several opportunities to informally present her research to key persons at the Broad Institute, including Dr. Todd R. Golub (Founding Member, Director of the Cancer Program) to help shape the direction of ongoing data analysis. Dr. Boehnke also had formal presentation opportunities, including sharing the results of the described project at the Broad Institute's Cancer Program meeting to gain valuable feedback on data analysis and planning of follow-up validation experiments as well as making new connections that may result in future collaborations.
As the data analysis presented in this report required processing of large data sets, Dr. Boehnke also took several courses offered to the MIT community, such as "intro to R" (organized by the Koch Institute BioMicro center) to gain skills R programming skills.

Professional development:
Workshops and conferences: Dr. Boehnke had planned to attend the Gordon Research Conference Drug Carriers in Medicine and Biology at Mt. Snow, VT this summer. However, due to COVID, the conference was canceled. Therefore, Dr. Boehnke took advantage of several conferences that had switched to online formatting. Dr. Boehnke has submitted abstracts that cover the funded work to the ACS National Meeting (Aug. 17-20) and the BMES Annual Meeting (Oct. 14-17). Dr. Boehnke has additionally signed up for a virtual professional grant writing workshop organized by the National Funding Foundation (Sept. 14) at the recommendation of her advisor, Prof. Hammond.

Seminars: Dr. Boehnke routinely attended, and will continue to attend, seminars at both MIT and the Broad Institute to further her experience in cancer biology and clinical genomics. Special emphasis was placed on seminars with a focus on pediatric, adolescent, and young adult cancers (e.g. medulloblastoma, sarcomas).

How were the results disseminated to communities of interest?

The results were shared with the MIT and Broad communities as described in the training and professional development section, above.
Additionally, the laboratory of the mentor, Dr. Paula Hammond, hosts several undergraduate researchers each summer from the MIT Summer Research Program (MSRP). MSRP seeks to increase diversity and prepare and recruit talented researchers and potential graduate students from underprivileged and underserved backgrounds. Specifically, as indicated on the MSRP website: "MSRP seeks to identify talented sophomores, juniors, and non-graduating seniors who might benefit from spending a summer on MIT's campus, conducting research under the guidance of MIT faculty members, postdoctoral fellows, and advanced graduate students. Students who participate in this program will be better prepared and motivated to pursue advanced degrees, thereby helping to sustain a rich talent pool in critical areas of research and innovation." Dr. Boehnke participates in this program annually to directly supervise an MSRP intern in the lab. This year, due to COVID restricting campus access, the program was held virtually, thus requiring a non lab-based project. As such, Dr. Boehnke and her intern, Jeandele Elliot from Howard University, carried out nanoPRISM data analysis to evaluate if cancer lineage and subtypes are predictive of nanoparticle uptake patterns. As part of the summer project, Jeandele was exposed to large datasets and multi-omics analysis approaches for the first time. The research findings from this project were also shared with the general MSRP cohort during formal presentations at the end of the summer session.

What do you plan to do during the next reporting period to accomplish the goals?

A 12 month no cost extension was granted due to COVID shutting down research at MIT starting March 2020. This significantly impaired progress toward Specific Aim 3. Therefore, this work will be carried out between now and July 2021. Specifically, therapy-loaded nanoparticles will be synthesized and characterized for drug loading and nanoparticle stability. These nanoparticles will then be used to evaluate *in vitro* cytotoxicity on the three cell lines identified in Specific Aim 2 prior to carrying out a PRISM viability screen (Major Tasks 1-3, Specific Aim 3).

4. IMPACT:

What was the impact on the development of the principal discipline(s) of the project?

The approach and findings described herein are the first report, to our knowledge, of correlating genomics with nanoparticle uptake to identify and construct genetic nanoparticle trafficking networks and identify biomarkers predictive of nanoparticle uptake. Moreover, the development and study of targeted nanocarriers in understudied diseases, such as cancers affecting children, adolescents, and young adults, has been previously limited to being studied in a small number of cell lines that do not capture the heterogeneity of the disease. By applying the large high throughput screen reported here, we were able to identify a pan-cancer biomarker that also appears to be correlated in the cell lines of these understudied cancers, pending further validation. Taken together, this new way of approaching nanoparticle study and design will enable a new way to engineer more effective and targeted nanocarriers by considering the genetic signatures of the target disease and leveraging therapeutic vulnerabilities. We are currently in the process of validating these findings, and communication of results is anticipated via conference presentations at the national meetings for the American Chemical Society and Biomedical Engineering Society this Fall as well as via publication of a manuscript currently in preparation.

What was the impact on other disciplines?

By bridging the gap between engineering targeted nanoparticles and cancer genomics, we have identified a new use of the established PRISM platform (Broad Institute). The PRISM screen has been expanded to enable flow-based sorting for target/biomarker identification in a non-drop out screen. This approach, which was described herein to identify nanoparticle-specific biomarkers, could be broadly applicable to cancer biologists to aid the identification of targets and validation of additional therapeutics, including other drug delivery modalities such as antibody drug conjugates, as well as target identification, such as of protein and peptide-based biologics.

This approach has been optimized with input from the PRISM team (Broad Institute) and shared with the Broad community to make them aware that flow-based PRISM screening is a possibility for target and mechanism identification.

What was the impact on technology transfer?

Nothing to Report.

What was the impact on society beyond science and technology?

Nothing to Report.

5. CHANGES/PROBLEMS:

Changes in approach and reasons for change

Nothing to Report.

Actual or anticipated problems or delays and actions or plans to resolve them

Delays due to COVID shutting down campus and halting research activities have already been detailed in the 12 month no cost extension.

Changes that had a significant impact on expenditures

Nothing to Report.

Significant changes in use or care of human subjects, vertebrate animals, biohazards, and/or select agents

Significant changes in use or care of human subjects

Not required/Nothing to Report.

Significant changes in use or care of vertebrate animals

Not required/Nothing to Report.

Significant changes in use of biohazards and/or select agents

Not required/Nothing to Report.

6. **PRODUCTS:** *List any products resulting from the project during the reporting period. If there is nothing to report under a particular item, state "Nothing to Report."*

- **Publications, conference papers, and presentations**

Journal publications.

Boehnke, N.; Dolph, K. J.; Juarez, V. M. Lanoha, J. M.; Hammond, P. T. "Electrostatic conjugation of nanoparticle surfaces with functional peptide motifs." *In revision*.
Acknowledgement of federal support: Yes

Zou, Y.*; Henry, W. S.*; Ricq, E. L.*; Graham, E. T.; Maretich, P.; Paradkar, S.; Phadnis, V. V.; Boehnke, N.; Deik, A. A.; Ferguson, B.; Wang, W.; Fairman, J.; Keys, H.; Dancik, V.; Clish, C. B.; Clemons, P. A.; Hammond, P. T.; Boyer, L. A. Weinberg, R. A.; Schreiber, S. L. "Plasmalogen plasticity promotes ferroptosis susceptibility and evasion." *Nature*, accepted.
Acknowledgement of federal support: Yes

Books or other non-periodical, one-time publications.

Not applicable/nothing to report.

Other publications, conference papers and presentations.

Not applicable/nothing to report.

- **Website(s) or other Internet site(s)**

Not applicable/nothing to report.

- **Technologies or techniques**

Technique: We have demonstrated that the previously established PRISM platform (Broad Institute) has now been expanded to enable flow-based sorting to enable target/biomarker identification in a non-drop out screen. This approach, which was described herein to identify nanoparticle-specific biomarkers, could be broadly applicable to the identification of targets and validation of additional therapeutics, including other drug delivery modalities such as antibody drug conjugates, as well as target identification, such as of protein and peptide-based biologics.

- **Inventions, patent applications, and/or licenses**

  Not applicable/nothing to report.

- **Other Products**

  Not applicable/nothing to report.

7. PARTICIPANTS & OTHER COLLABORATING ORGANIZATIONS

What individuals have worked on the project?

Name: Natalie Boehnke
Project Role: Postdoc (PI)
Researcher Identifier (e.g. ORCID ID): 0000-0002-3468-2033
Nearest person month worked: 12

Contribution to Project: Dr. Boehnke designed and carried out all experiments and associated data analysis, as designated in the SoW.
Funding Support: -

Has there been a change in the active other support of the PD/PI(s) or senior/key personnel since the last reporting period?

Nothing to report.

What other organizations were involved as partners?

Organization name: Broad Institute of MIT and Harvard
Location of Organization: Cambridge, MA
Partner's contribution to the project: collaboration
During the reporting period, we collaborated with the PRISM platform at the Broad Institute to carry out the proposed PRISM screen to profile nanoparticle – cell interactions (see letter of support in grant application). The PRISM platform provided us with the pooled and barcoded cells for testing carried out at MIT. The PRISM team also carried out DNA barcode deconvolution (amplification, sequencing) of the cell lysates that were handed to them post flow sorting.

8. SPECIAL REPORTING REQUIREMENTS

COLLABORATIVE AWARDS: *not applicable*

QUAD CHARTS: *not applicable*

9. APPENDICES:

References cited:

(1) Boehnke, N., Correa, S., Hao, L., Wang, W., Straehla, J. P., Bhatia, S. N., and Hammond, P. T. (2020) Theranostic Layer-by-Layer Nanoparticles for Simultaneous Tumor Detection and Gene Silencing. *Angew Chem Int Ed Engl 59*, 2776-2783.

(2) Kwon, E. J., Dudani, J. S., and Bhatia, S. N. (2017) Ultrasensitive tumour-penetrating nanosensors of protease activity. *Nature Biomedical Engineering 1*.

(3) Shi, J. J., Kantoff, P. W., Wooster, R., and Farokhzad, O. C. (2017) Cancer nanomedicine: progress, challenges and opportunities. *Nature Reviews Cancer 17*, 20-37.

(4) Hamblett, K. J., Jacob, A. P., Gurgel, J. L., Tometsko, M. E., Rock, B. M., Patel, S. K., Milburn, R. R., Siu, S., Ragan, S. P., Rock, D. A., Borths, C. J., O'Neill, J. W., Chang, W. S., Weidner, M. F., Bio, M. M., Quon, K. C., and Fanslow, W. C. (2015) SLC46A3 Is Required to Transport Catabolites of Noncleavable Antibody Maytansine Conjugates from the Lysosome to the Cytoplasm. *Cancer Research 75*, 5329-5340.

(5) Tsui, C. K., Barfield, R. M., Fischer, C. R., Morgens, D. W., Li, A., Smith, B. A. H., Gray, M. A., Bertozzi, C. R., Rabuka, D., and Bassik, M. C. (2019) CRISPR-Cas9 screens identify regulators of antibody-drug conjugate toxicity. *Nature Chemical Biology 15*, 949-+.

(6) Li, G. M., Guo, J., Shen, B. Q., Yadav, D. B., Sliwkowski, M. X., Crocker, L. M., Lacap, J. A., and Phillips, G. D. L. (2018) Mechanisms of Acquired Resistance to Trastuzumab Emtansine in Breast Cancer Cells. *Molecular Cancer Therapeutics 17*, 1441-1453.

(7) Zhao, Q., Zheng, B., Meng, S. Q., Xu, Y., Guo, J., Chen, L. J., Xiao, J., Zhang, W., Tan, Z. R., Tang, J., Chen, L., and Chen, Y. (2019) Increased expression of SLC46A3 to oppose the progression of hepatocellular carcinoma and its effect on sorafenib therapy. *Biomedicine & Pharmacotherapy 114*.